Molecular Biology of the Cell
Vol. 18, 2795–2804, August 2007

A Developmentally Regulated Chaperone Complex for the Endoplasmic Reticulum of Male Haploid Germ Cells

Marcel van Lith,* Anna-Riikka Karala,† Dave Bown,* John A. Gatehouse,* Lloyd W. Ruddock,† Philippa T.K. Saunders,‡ and Adam M. Benham*

*Department of Biological and Biomedical Sciences, University of Durham, Durham, DH1 3LE, United Kingdom; †Biocenter Oulu and Department of Biochemistry, University of Oulu, 90014 Oulu, Finland; and ‡Medical Research Council Human Reproductive Sciences Unit, The Queen's Medical Research Institute, Edinburgh, EH16 4TJ, United Kingdom

Submitted February 20, 2007; Revised April 23, 2007; Accepted May 4, 2007
Monitoring Editor: Sean Munro

Glycoprotein folding is mediated by lectin-like chaperones and protein disulfide isomerases (PDIs) in the endoplasmic reticulum. Calnexin and the PDI homologue ERp57 work together to help fold nascent polypeptides with glycans located toward the N-terminus of a protein, whereas PDI and BiP may engage proteins that lack glycans or have sugars toward the C-terminus. In this study, we show that the PDI homologue PDILT is expressed exclusively in postmeiotic male germ cells, in contrast to the ubiquitous expression of many other PDI family members in the testis. PDILT is induced during puberty and represents the first example of a PDI family member under developmental control. We find that PDILT is not active as an oxido-reductase, but interacts with the model peptide Δ-somatostatin and nonnative bovine pancreatic trypsin inhibitor in vitro, indicative of chaperone activity. In vivo, PDILT forms a tissue-specific chaperone complex with the calnexin homologue calmegin. The identification of a redox-inactive chaperone partnership defines a new system of testis-specific protein folding with implications for male fertility.

INTRODUCTION

Protein disulfide isomerase (PDI) catalyzes the formation, isomerization and reduction of disulfide bonds in the endoplasmic reticulum (ER). More than 17 mammalian PDI homologues have been identified all characterized by the presence of one or more thioredoxin folds (Ellgaard and Ruddock, 2005). PDI itself contains four of these thioredoxin domains: two with the thioredoxin redox active site CXXC (designated a-type domains) and two domains lacking the active site (designated b-type domains). The b-type domains lack redox activity, but have either a structural function or are involved in substrate recognition and binding (Klappa *et al.*, 1998a). In PDI, these domains have an a-b-b′-a′ organization. PDIp, ERp57, and PDILT share the same domain structure with PDI, but various other configurations of thioredoxin domains exist in other PDI family members, with most PDIs containing at least one a-type domain with an intact active site motif (Ellgaard and Ruddock, 2005).

PDI homologues are not functionally equivalent, as shown by differences in their ability to complement a yeast strain deficient for PDI (Gunther *et al.*, 1993; Kramer *et al.*, 2001). Furthermore, the different PDI family members interact with discrete sets of substrates. PDI catalyzes in vitro redox reactions in a wide variety of substrates, including bovine pancreatic trypsin inhibitor (BPTI), insulin, and ribonuclease (Weissman and Kim, 1993; Zheng and Gilbert, 2001). PDI also displays chaperone activity toward nondisulfide bond–containing substrates (Cai *et al.*, 1994) and forms the noncatalytic subunit in prolyl 4-hydroxylase (Koivu *et al.*, 1987) and microsomal triglyceride transfer complex (Wetterau *et al.*, 1990). ERp57 interacts with a specific set of glycosylated proteins that are recruited via its interaction with the lectins calnexin/calreticulin (Oliver *et al.*, 1997; Jessop *et al.*, 2007) and is a component of the major histocompatibility complex (MHC) class I loading complex (Lindquist *et al.*, 1998; Dick *et al.*, 2002). ERp72 has been found in association with a number of immature or unfolded proteins, including MHC class II and thyroglobulin (Schaiff *et al.*, 1992; Kuznetsov *et al.*, 1994) and has been implicated in ER retention of misfolded proteins (Forster *et al.*, 2006). The pancreas-specific PDIp binds unfolded proteins and specifically recognizes tryptophan and tyrosine residues in substrates (Klappa *et al.*, 1998b; Ruddock *et al.*, 2000). Therefore, multiple PDI homologues may be required for substrate-specific folding.

Two PDI-like proteins, ERp44 and PDILT, have ER lumenal a-type domains, but lack the canonical active site motif, whereas ERp27 and ERp28 are devoid of a-type domains (Ferrari *et al.*, 1998; Anelli *et al.*, 2002; van Lith *et al.*, 2005; Alanen *et al.*, 2006). Most PDI family members are ubiquitously expressed, although a few PDI family members such as endoPDI, PDIp, and PDILT have a restricted tissue distribution. PDIp expression is mostly limited to the pancreas (Desilva *et al.*, 1996; Dias-Gunasekara *et al.*, 2005). Although PDIp may have overlapping substrate specificities with PDI, it could serve as a specific folding catalyst for a

This article was published online ahead of print in *MBC in Press* (http://www.molbiolcell.org/cgi/doi/10.1091/mbc.E07–02–0147) on May 16, 2007.

Address correspondence to: Adam Benham (adam.benham@durham.ac.uk).

Abbreviations used: BPTI, bovine pancreatic trypsin inhibitor; endoH, endoglycosidase H; IAA, iodo-acetic acid; MHC, major histocompatibility complex; PDI, protein disulfide isomerase; PDILT, protein disulfide isomerase-like protein of the testis.

subset of pancreatic secretory proteins (Ruddock *et al.*, 2000). EndoPDI/ERp46, with three CxxC thioredoxin motifs, is highly expressed in endothelial cells where it has a protective role during hypoxia (Sullivan *et al.*, 2003). The third PDI family member with restricted tissue expression is PDILT.

We have recently identified PDILT as a PDI homologue that is specifically expressed in testis (van Lith *et al.*, 2005). The testis has two distinct compartments: the seminiferous tubules, which contain differentiating germ cells supported by somatic Sertoli cells, and an interstitium containing Leydig cells, peritubular cells, and blood vessels. Germ cell maturation (spermatogenesis) is a complex process; during the first phase, diploid spermatogonia undergo rounds of mitotic replication before entering a second, lengthy, meiotic prophase that culminates in two rounds of cell division to yield haploid spermatids. During the third phase, known as spermiogenesis, the spermatids undergo extensive remodeling characterized by loss of somatic histones, DNA compaction, cessation of DNA transcription, and development of a flagellum (Hess, 1990). Within the seminiferous epithelium the germ cells at different phases of maturation are arranged in constant associations known as "stages" with the diploid spermatogonia at the periphery of the tubules and the most mature, haploid, elongate spermatids proximal to the lumen (Hess, 1990; Russell *et al.*, 1990).

In the present study, we set out to determine PDILT expression and function in the testis. Although calnexin interacts with ERp57 to support disulfide bond formation in newly synthesized glycoproteins in somatic cells (Oliver *et al.*, 1997), we identify PDILT as a partner for the testis-specific calnexin homologue calmegin in postmeiotic male germ cells. Our data suggest that PDILT-calmegin complexes are required as a specialized chaperone system for spermatogenesis-specific proteins during the final stages of germ cell maturation.

MATERIALS AND METHODS

Cell Lines, Tissues, and Antibodies

Human cervical carcinoma HeLa cells were maintained in minimal Eagle's medium (Invitrogen, Carlsbad, CA) supplemented with 8% fetal calf serum (Sigma, St. Louis, MO), 2 mM glutamax, 100 U/ml penicillin, and 100 μg/ml streptomycin (Invitrogen).

Tissues for immunoprecipitation/Western blot analysis and immunohistochemistry were obtained from rats (SD) and mice (C57/B6 or CD1). Sections of testes from human, stump-tailed macaque, and common marmoset were from blocks of fixed tissue held in an archive at the Human Reproductive Sciences Unit Edinburgh.

The anti-HA (HA-7; Sigma), anti-myc (9B11; Cell Signaling, Beverly, MA), anti-ERp72 (Calbiochem, La Jolla, CA) and anti-BiP (H-129; Santa Cruz Biotechnology, Santa Cruz, CA) antibodies were commercially available. The PDILT antiserum was raised against purified recombinant His-tagged PDILT; this antiserum was used in all experiments, except where noted. The anti-peptide PDILT antiserum was raised against the PDILT peptide RQKLINDSTNKQELN coupled to hemocyanin and was a kind gift from Dr. L. Ellgaard (University of Copenhagen, Denmark). The polyclonal antiserum against PDI has been described (Benham *et al.*, 2000), and the mAb against PDI was obtained from Affinity BioReagents (Golden, CO). The anti-ERp57 antiserum was a kind gift from Prof. N. Bulleid (University of Manchester, England). The calmegin antiserum was a kind gift from Prof. Y. Nishimune (The Research Institute of Microbial Diseases, Osaka, Japan). The calnexin antiserum was a kind gift from Prof. I. Braakman (University of Utrecht, The Netherlands).

Constructs

Construction of human PDILT with a C-terminal myc-tag has been described previously (van Lith *et al.*, 2005). The PDILT cysteine-to-alanine mutants were generated from this construct using Quik Change Site-Directed Mutagenesis kit (Stratagene, La Jolla, CA) using primers GTCAGAGCCCATCAGCGCCAAAGGAGTGGTTGAATC/GATTCAACCACTCCTTTGGCGCTGATGGGCTCTGAC (PDILT C135A) and GCACCCTGGTCTAAAAAGGCCAAGATGCTGTTCCCAC/GTGGGAACAGCATCTTGGCCTTTTTAGACCAGGGTGC (PDILT C420A). For biophysical analysis, mature PDILT (S21-L584) was cloned into pLWRP51, a modified pET23b vector (Novagen, Madison, WI), which encodes an N-terminal His tag (MHHHHHHM) before the first amino acid of the protein sequence, using the primers TTTTTTTCATATGTCACCAGAGGTTAACGCCGGTG and TTTTTTTTGGATCCTTATTAAAGTTCTTCCTTGACTTTTGGTTTCTTCTTTTGC. The PDILT-HA construct was a kind gift from Dr. L. Ellgaard. All plasmids generated were verified by sequencing.

Transfections

Transfections with Lipofectamine 2000 (Invitrogen) were done according to the manufacturer's instructions. Subconfluent cells in 6-cm dishes were washed with Hanks' balanced salt solution and Optimem and transfected with 1 μg of DNA for 6 h in the presence of Optimem serum-free medium. After 6 h the cells were washed and returned to normal growth medium. The cells were analyzed 24 h after transfection.

RNA Isolation and RT-PCR

Total RNA from rat tissues was extracted using TRI reagent (Sigma) according to the manufacturer's instructions. The RNA concentration was determined by spectrophotometry to ensure equal total RNA input. RT-PCR was performed with the AccessQuick kit (Promega, Madison, WI) using 50 ng RNA on a Peltier Thermal Cycler (MJ Research, Waltham, MA). Sense and antisense primers were designed on different exons to exclude amplification of contaminating genomic DNA: PDILT (set 1), CATCGTTGGCTTCTTCCAG and TATTTTGGAATCTCTTCACTGG; PDILT (set 2), CCATGTGCTCAAGCAGGAAC and CACTCAGAAACTGATGTCAGGAC; calmegin, CACCTCAACCTATAGGAGAAG and CTTCATCTCATCCTCTGATCC; PDI, AAGGAATATACAGCTGGCAG and CCTTCTTCAGGCCAAAGAAC; and actin, CCACACCTTCTACAATGAGC and ACTCCTGCTTGCTGATCCAC.

PCR products were analyzed on 1% agarose gels.

Immunoprecipitations and Western Blotting

Cells and tissues were lysed in 1% Triton X-100, 50 mM Tris (pH 8.0), 150 mM NaCl, and 5 mM EDTA, supplemented with 20 mM iodo-acetic acid (IAA) and protease inhibitors. Postnuclear lysates were incubated with protein A Sepharose beads (Sigma) and antisera for 1–2 h at 4°C. After extensive washing of the beads, immunoprecipitated proteins were eluted by boiling in sample buffer and analyzed by 8% SDS-PAGE. Proteins were transferred to polyvinylidene difluoride membranes (Millipore, Bedford, MA) at 150 mA for 2 h. The membranes were blocked in Tris-buffered saline Tween (TBST) with 8% milk, followed by incubation with primary antibody at the following concentrations: 1:2000 anti-myc and anti-HA, 1:10,000 anti-PDILT, and 1:1000 anti-PDI and anti-calmegin. After washing three times with TBST, the membranes were incubated with secondary antibodies (DAKO, High Wycombe, Bucks., United Kingdom), washed, and visualized by electrochemiluminescence (ECL; Amersham/GE Healthcare, Little Chalfont, United Kingdom) and exposure to film (Eastman Kodak, Rochester, NY). Protein markers were from Bio-Rad.

Endoglycosidase H Treatment

Samples were treated with endoglycosidase H (endoH) according to the manufacturer's protocol (New England Biolabs, Beverly, MA). Briefly, lysates cleared by centrifugation were β2-mercaptoethanol–reduced and SDS-denatured followed by incubation without or with endoH in 50 mM sodium citrate (pH 5.5) at 37°C for 16 h and analyzed by SDS-PAGE.

Immunohistochemistry

Testicular tissues were fixed in Bouins solution, processed into paraffin wax according to standard procedures and cut in 4-μm-thick sections onto polylysine slides (VWR Scientific Products, West Chester, PA). Wax was removed with Histoclear (Agar Scientific, Stansted, United Kingdom), and the tissue was rehydrated in sequential washing steps from 100 to 70% ethanol. Endogenous peroxidase activity was blocked with 1% hydrogen peroxide in methanol. Antigen retrieval was done by incubating the slides in 10 mM sodium citrate at 90°C for 30 min. After a blocking step in phosphate-buffered saline (PBS) with 5% goat serum and 0.2% bovine serum albumin (BSA), the sections were incubated with primary antibodies in PBS with 0.2% BSA. Primary antibodies were detected with the ABC kit (DAKO) followed by developing with 3,3′-diaminobenzidine (DAB; Sigma). Sections were counterstained with hematoxylin. Slides were mounted with 1,3-diethyl-8-phenylxanthine (DPX; Agar Scientific) and analyzed with an inverted microscope (Axiovert 10, Zeiss, Thornwood, NY).

Purification of Human Recombinant PDILT

His-tagged PDILT was expressed in the *Escherichia coli* strain BL21 (DE3) pLysS in LB medium at 37°C by inducing with 1 mM isopropyl β-D-thiogalactoside at an OD600 of 0.3 for 4 h. After pelleting at 8000 rpm for 10 min, the pellet was resuspended in one-tenth volume of 20 mM sodium phosphate (pH 7.3) with 10 μg/ml DNase (Roche, Indianapolis, IN). The cells were lysed by

freeze-thawing twice, and the insoluble material was collected by centrifugation (9000 rpm for 20 min). The pellet was washed twice with 20 ml of 50 mM Tris, 10 mM EDTA, 0.5% Triton X-100 (pH 8.0), twice with distilled water, and centrifuged at 9000 rpm for 20 min between each wash. PDILT was recovered from the washed pellet by solubilizing in 20 ml of 5 M guanidine hydrochloride/50 mM Tris (pH 8.75), with the insoluble material removed by centrifugation at 9000 rpm for 20 min. The soluble fraction was incubated in 10 mM dithiothreitol (DTT) at room temperature for 30 min. Excess DTT was removed by gel filtration using a PD-10 column (GE Healthcare) which had been pre-equilibrated in 5 M guanidine hydrochloride, 0.2 M sodium phosphate (pH 7.0). Solubilized His-PDILT was loaded onto a His-Trap column (GE Healthcare) and refolded on-column by a linear buffer exchange from 3 M guanidine/0.2 M sodium phosphate (pH 7.0) to 0.2 M sodium phosphate (pH 7.0) over 4 h. PDILT was eluted from the column with 50 mM EDTA, 20 mM sodium phosphate (pH 7.0).

Purified Rat PDI was a gift from N. Bulleid.

Biophysical Analysis

Far UV circular dichroism spectra were obtained on a Jasco J810 Spectropolarimeter (Easton, MD). Data were collected using 0.1 mg/ml PDILT at 25°C as an average of eight scans, using a cell with a path length of 0.1 cm, measured at a scan speed of 20 nm/min, a spectral bandwidth of 1.0 nm, and a time constant of 0.5 s. The maximum HT voltage was below 600 V.

Fluorescence spectra were collected on a PerkinElmer Life Sciences LS50 spectrophotometer (Boston, MA) using a 1-ml cuvette. Data were collected at 25°C as an average of four scans, excitation at 280 nm, emission at 300–400 nm, slit widths of 5 nm, and a scan speed of 200 nm/min. Protein stocks were diluted ~20-fold to a final concentration of 2 μM into 0.2 M phosphate buffer, pH 7.0, containing 0–6 M guanidine hydrochloride and equilibrated for 5 min at 25°C before fluorescence spectra were recorded. All spectra were corrected for the blank spectra with no protein added. The fluorescence parameter examined to observe the effects of guanidine hydrochloride on protein structure was the ratio of the average fluorescence intensity 2 nm either side of the λ_{max} for native protein to the average fluorescence intensity over the range 320–400 nm. This parameter was chosen because it is independent of concentration and less dependent on the direct effects of guanidine hydrochloride on tryptophan fluorescence.

Oxido-reductase Assays

For the insulin-reduction assay, human insulin (Sigma) at a final concentration of 0.17 mM was incubated with 1 μM PDILT or PDI in the presence of 5 mM DTT. Precipitation of the insulin B chain was monitored by measuring OD600 at 5-min intervals after addition of insulin.

To monitor protein oxidation and isomerization, 70 μM of recombinant bovine pancreatic trypsin inhibitor (BPTI) in 0.1 M Tris buffer, pH 7.5, or 0.1 M phosphate buffer, pH 6.0, both containing 1 mM EDTA, 2 mM reduced glutathione (GSH), and 0.5 mM oxidized glutathione was incubated with and without 10 μM of PDILT. Disulfide bond formation of BPTI was monitored by trapping thiol-disulfide exchange by treating with 1.1 M iodoacetamide, desalting the sample, and analyzing it by electrospray mass spectrometry (Micromass, Manchester, United Kingdom).

The protein oxidation assay using a fluorescent decapeptide with 3.2 μM peptide substrate and 0.2 μM PDILT has been described (Ruddock *et al.*, 1996). Deglutathionylation activity was monitored as described previously (Peltoniemi *et al.*, 2006), using 0.2 μM PDILT in the presence of 1 mM GSH and 5 μM substrate peptide. Glutathionylation activity was determined as described previously (Peltoniemi *et al.*, 2006), using 0.2 μM PDILT and 5.4 μM substrate peptide.

Peptide-binding Assay

Cell extracts from *E. coli* BL21 (DE3) pLysS were prepared by repeated freeze-thawing. Bolton-Hunter ^{125}I-labeling of Δ-somatostatin (AGSKNFFWKTFSS) was performed as recommended by the manufacturer (Amersham Pharmacia Biotech, Piscataway, NJ). Cross-linking was performed using the homobifunctional cross-linking reagent disuccinimidyl glutarate (Sigma) as described (Klappa *et al.*, 1998a). As a positive control an *E. coli* lysate expressing ERp27 (Alanen *et al.*, 2006) was used. This lysate was prepared as detailed for the purification of PDILT, except that because ERp27 is solubly expressed, the soluble postlysis material was used.

RESULTS

Biophysical Characterization of PDILT

PDILT shares almost 50% sequence similarity with PDI, with the most notable differences being the altered active site motifs in PDILT (SXXS and SXXC) and a free cysteine at position 135 in the first catalytic domain. C135 is conserved in PDILT between species, but is not found in other PDI family members. As PDI has both redox and chaperone-like properties, we wanted to see whether these functions were retained in PDILT. Therefore, we purified and refolded a His-tagged version of PDILT from a bacterial lysate to near-purity as shown on a Coomassie-stained SDS-PAGE gel (Figure 1A). Mass spectrometry analysis of the purified protein gave the correct mass (65612.5 Da) for a single sodium adduct of the protein. The far-UV circular dichroism spectrum suggested that PDILT was structured and contained a significant amount of α-helix and β-sheet (Figure 1B). Mature PDILT contains three tryptophans, and the fluorescence spectra of PDILT under nondenaturing conditions gave a λ_{max} of 334 nm (Figure 1C), indicative of a tryptophan residue being in a hydrophobic environment. On addition of 6 M guanidinium chloride the fluorescence spectra of PDILT had a λ_{max} of 354 nm, indicative of a denatured protein. Fluorescence-based denaturation curves for PDILT showed a multiple-phase transition from the native to the denatured state (Figure 1D), similar to that observed for PDI (Morjana *et al.*, 1993). The midpoint of the fluorescence change between 0 and 6 M guanidinium chloride was around 3.5 M, higher than that of any domain of PDI, indicating that the purified PDILT was structured.

Human PDILT contains two cysteine residues: one in the catalytic site of the second catalytic domain (C420) and one away from the catalytic site in the first catalytic domain, but at a position suitable for PDI-substrate interactions (C135). Under nondenaturing conditions PDILT has a free sulfhydryl content of 2.1, as determined by the Ellman's reagent assay (data not shown), implying that both cysteines are solvent accessible. In addition, when lysates from HeLa cells transfected with PDILT were analyzed by nonreducing SDS-PAGE, PDILT was engaged in disulfide-linked complexes (Figure 1E, lane 1). Replacement of either cysteine with alanine resulted in the loss of some, but not all complexes, showing that each cysteine mediates distinct disulfide-linked complexes (Figure 1E, lanes 2 and 3). As expected, mutation of both cysteines abolished all disulfide-linked PDILT complexes (Figure 1E, lane 4). Thus, the PDILT cysteines are solvent exposed, both in vitro and in vivo.

Because both cysteines of PDILT are solvent exposed, we next examined if PDILT had oxido-reductase activity. PDI catalyzes a wide range of thiol-disulfide exchange reactions, including reduction of disulfides, oxidation of dithiols to a disulfide, and reductive removal of a glutathione moiety from a protein-glutathione mixed disulfide (Ruddock *et al.*, 1996; Peltoniemi *et al.*, 2006). First, we used an insulin reduction assay (Holmgren, 1979) to establish whether PDILT had reductase activity. When PDI was incubated with insulin in the presence of DTT, the insulin B chain rapidly precipitated as expected (Figure 1F, PDI). In contrast, PDILT did not display any reductase activity over the nonenzymatic reduction of insulin alone (Figure 1F, compare PDILT vs. insulin), suggesting that PDILT is not a conventional disulfide oxidoreductase. Similarly, PDILT does not show any peptide oxidation activity toward a decapeptide substrate (Ruddock *et al.*, 1996), nor does it show any deglutathionylation activity toward a glutathionylated octapeptide (Peltoniemi *et al.*, 2006) nor glutathionylation activity toward a nonglutathionylated version of the same octapeptide (data not shown).

In contrast to these results, PDILT-substrate interactions were observed in a BPTI refolding assay. BPTI has been widely used to study PDI-catalyzed protein refolding (Weissman and Kim, 1993). Reduced BPTI is soluble, as is purified PDILT, but when they were combined, a precipitate formed rapidly. Analysis of the precipitate by SDS-PAGE showed that it contained both proteins, indicating a PDILT-

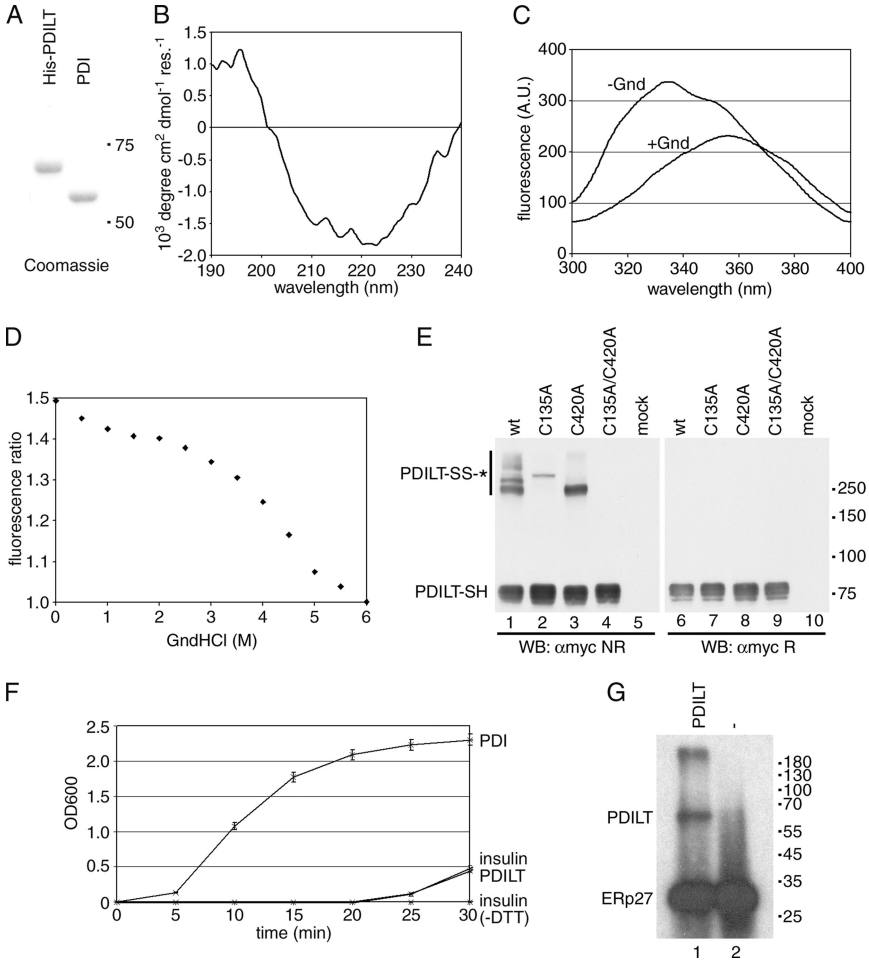

Figure 1. PDILT has chaperone-like properties. (A) Purified human His-tagged PDILT and purified rat PDI were analyzed by SDS-PAGE and Coomassie staining. (B) Far-UV circular dichroism spectrum of purified recombinant human PDILT. (C) Fluorescence spectra of purified human His-tagged PDILT under native (−Gnd) and denaturing conditions (+Gnd). (D) Guanidine hydrochloride denaturing curve of purified human His-tagged PDILT. Shown is the ratio of the average fluorescence intensity at 332–336 nm (peak of native protein) to that at 320–400 nm. (E) HeLa cells were mock-transfected or transfected with myc-tagged wild-type PDILT or the PDILT cysteine mutants as indicated. Lysates of these transfectants were analyzed by nonreducing (lanes 1–5) and reducing (lanes 6–10) SDS-PAGE. Monomeric PDILT (PDILT-SH) and PDILT in disulfide-linked complexes (PDILT-SS-*) are indicated. Molecular weights in kDa are indicated on the right-hand side. (F) Human insulin, 0.17 mM, was incubated with DTT only (insulin) or DTT with 1 μM enzyme (PDI or PDILT) in PBS. Insulin without DTT (insulin-DTT) was indistinguishable from PBS. The OD600 was monitored over 30 min to follow precipitation of the insulin B chain. (G) Extracts of *E. coli* expressing ERp27 were incubated with ^{125}I-labeled Δ-somatostatin with (lane 1) or without (lane 2) 2 μg recombinant PDILT. After cross-linking with disuccinimidyl glutarate, the samples were analyzed by SDS-PAGE.

BPTI interaction (data not shown). Because PDI is able to interact with peptides and proteins that do not contain cysteines, we next examined whether PDILT engages in similar interactions by using a Δ-somatostatin cross-linking assay. The 14-amino acid peptide Δ-somatostatin has previously been used to examine peptide/nonnative protein-binding sites in other PDI family members, including PDI (Klappa *et al.,* 1998a), PDIp (Klappa *et al.,* 1998b), and ERp27 (Alanen *et al.,* 2006). When radiolabeled Δ-somatostatin is added to suitable lysates, specific cross-linking with these PDI family members can be observed by autoradiography of SDS-PAGE gels. When PDILT was used in the Δ-somatostatin assay, a weak band was observed at the expected position of PDILT in an *E. coli* lysate that had 2 μg of purified PDILT added to it (Figure 1G, lane 1). These bacteria expressed human ERp27 as an internal control. Because the PDILT band was not visible in the control samples (Figure 1G, lane 2), this shows that PDILT interacts with Δ-somatostatin independently of substrate cysteines.

Expression of PDILT Is Restricted to a Subset of Germ Cells

To gain further insight into the function of PDILT in vivo, we raised a polyclonal antiserum against recombinant purified human PDILT. The antiserum specifically recognized both transfected PDILT in HeLa cells (Figure 2A) and endogenous PDILT in mouse testis (Figure 2B). The antiserum did not detect PDILT in nontesticular tissues (Figure 2B, top panel), whereas PDI and calnexin were detected in all tissues examined (Figure 2B, bottom panel), corroborating the testis-specific expression of PDILT reported previously (van Lith *et al.,* 2005).

Having demonstrated the specificity of the PDILT antiserum, we used immunohistochemistry on rat testis sections counterstained with hematoxylin to determine the cellular

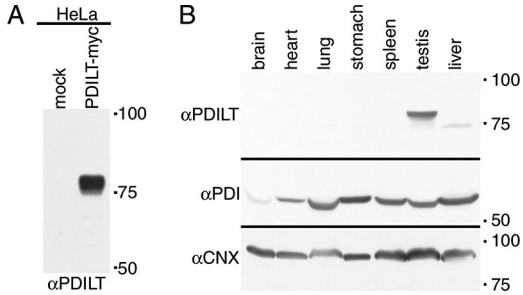

Figure 2. Specificity of the PDILT antiserum. (A) Lysates from HeLa cells transfected with PDILT-myc or an irrelevant myc construct were analyzed by Western blotting with a rabbit antiserum raised against purified recombinant His-tagged human PDILT. (B) Equal amounts (in mg of tissue) of murine tissue lysates were analyzed by Western blotting with a rabbit antiserum raised against purified recombinant His-tagged human PDILT (top), anti-PDI (middle), and anti-calnexin (bottom).

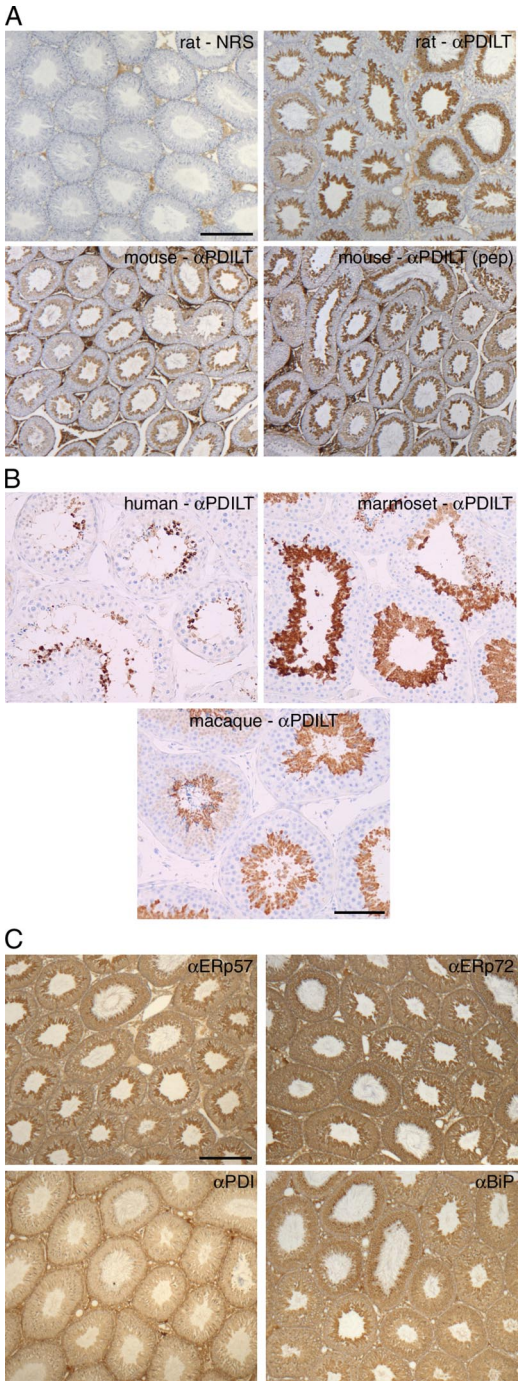

Figure 3. Expression of PDILT is germ cell specific. (A) Sections from rat testis counterstained with hematoxylin (blue) were immunostained with normal rabbit serum (NRS) or an anti-PDILT serum raised against recombinant PDILT at a dilution of 1:8000 (top panels). The PDILT staining pattern (brown) is similar for mouse testis (bottom left) or when using a serum raised against an internal PDILT peptide at 1:1000 (bottom right). Scale bar, 200 μm. (B) Testis sections from human, macaque, and marmoset were immunostained for PDILT. Although a single population of PDILT-positive germ cells occupied the full circumference of the tubule in macaque, the staining on human and marmoset was more heterogenous consistent with the existence of tubules containing more than one stage of spermatogenesis in a single cross section. Scale bar, 100 μm. (C) Rat testis sections were immunostained for ERp57, ERp72, PDI, and BiP (brown). Expression of these proteins was observed throughout the seminiferous epithelium. Scale bar, 200 μm.

site of PDILT expression. The preimmune serum showed minor staining in the interstitial areas of rat testis due to residual trapped serum (Figure 3A, rat-NRS) and was indistinguishable from secondary antibody alone (data not shown). In contrast, the anti-PDILT serum intensely stained populations of germ cells in the seminiferous tubules (Figure 3A, rat-αPDILT). The immunostaining pattern was essentially the same for mouse testis (Figure 3A, mouse-αPDILT) and when using the antiserum raised against a PDILT peptide [Figure 3A, mouse-αPDILT (pep)]. PDILT expression was also restricted to germ cells in testis from human, macaque, and marmoset (Figure 3B). Although in rat, mouse, and macaque, cross-sections of individual tubules are characterized as containing a single grouping (spermatogenic stage) of germ cells (Hess, 1990), the organization of spermatogenesis in human and the common marmoset is more complex, and tubule cross-sections contain germ cell complements typical of a mixture of stages (Schulze *et al.*, 1986; Millar *et al.*, 2000). The restricted expression pattern of PDILT to a subset of germ cells was in stark contrast with the expression patterns of other PDI family members PDI, ERp57, and ERp72 or the ER chaperone BiP. Although expression levels varied between the different cell types within the seminiferous tubules, expression of these other PDI family members was ubiquitous throughout the seminiferous epithelium (Figure 3C). Thus, PDILT is expressed in testis of multiple mammalian species and in contrast to other PDI family members, its expression is restricted to a subset of testicular germ cells.

PDILT Is Expressed in Postmeiotic Germ Cells

Closer examination of adult rat testis sections showed that PDILT was present in the most mature germ cells, located around the seminiferous tubule lumen (Figure 4A). When evaluated using the standard spermatogenic staging scheme (Figure 4B), it was apparent that immunopositive staining was first detectable in haploid round spermatids found at stage VII. In all species examined, the onset of PDILT expression commenced upon completion of meiotic prophase. Thereafter, in the rat PDILT was present in the cell body of all subsequent round and elongating spermatids (Figure 4A, stages IX, XI, and XIV). PDILT was not detected in spermatozoa in the epididymis or in the ejaculate (data not shown; Ellerman *et al.*, 2006), consistent with the finding that PDILT was not found in the nuclei of the spermatozoa but could be detected in apical and basal residual bodies (Figure 4A, stage XI) that are left behind when spermatozoa are released (Clermont *et al.*, 1987). The germ cells to which PDILT was localized are summarized on a diagram that shows the germ cells associations found in the different stages of spermatogenesis in the rat (Figure 4B).

PDILT Expression Is under Developmental Control

As PDILT was first seen at the round spermatid stage, we asked whether the onset of PDILT expression coincides with the appearance of differentiating germ cells during the first wave of spermatogenesis in development. Total RNA, isolated from rat testes at different ages, was used for RT-PCR to determine the expression of PDILT with age. A cDNA containing the coding region of PDILT gave a product of expected size (Figure 5A, PDILT 1). No product was observed when using RNA derived from testes of 2- and 15-d-old rats, demonstrating that PDILT was not expressed in somatic cells that make up the bulk of the testes at these ages. PDILT mRNA was detected in testis from day 30 and reached adult levels from day 45 onward. RNA from liver of a 58-d-old rat served as negative control (Figure 5A, PDILT

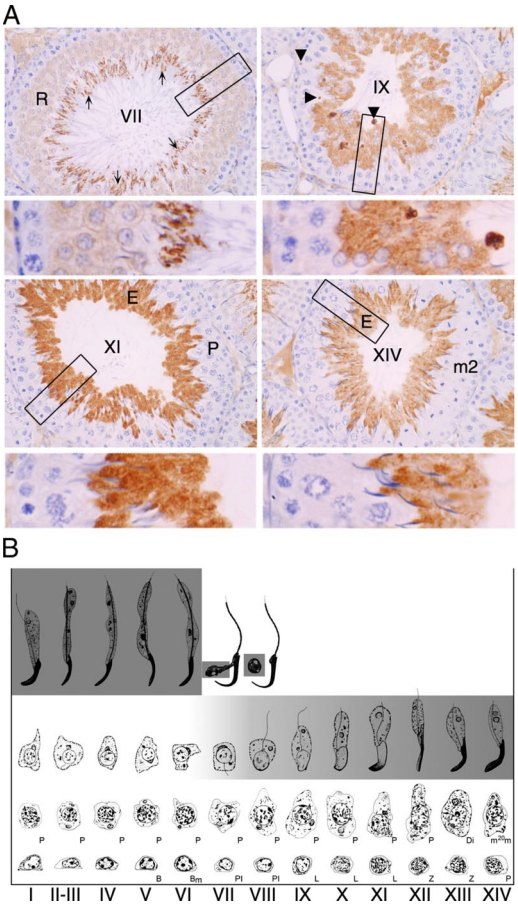

Figure 4. Germ cell expression of PDILT from stage VII. (A) Rat testis sections immunostained with anti-PDILT from Figure 3A were imaged at higher magnification. Four representative sections from stages VII, IX, XI, and XIV of the rat spermatogenic cycle are shown. A higher detailed section, indicated by a box, is shown below each stage. Round spermatids (R), elongate spermatids (E), and immunonegative pachytene spermatocytes (P) and germ cells undergoing meiotic division (m2) are indicated. At stage VII mature elongate spermatids ready for release are indicated by arrows. At stage IX immunopositive staining was particularly intense in small areas (arrowheads) that are likely to be the residual cytoplasmic remnants from spermatozoa released at stage VII. (B) A staging diagram showing the germ cell associations characteristic of the spermatogenic cycle (Russell *et al.*, 1990) summarizes the expression levels of PDILT (gray shading) in the adult rat.

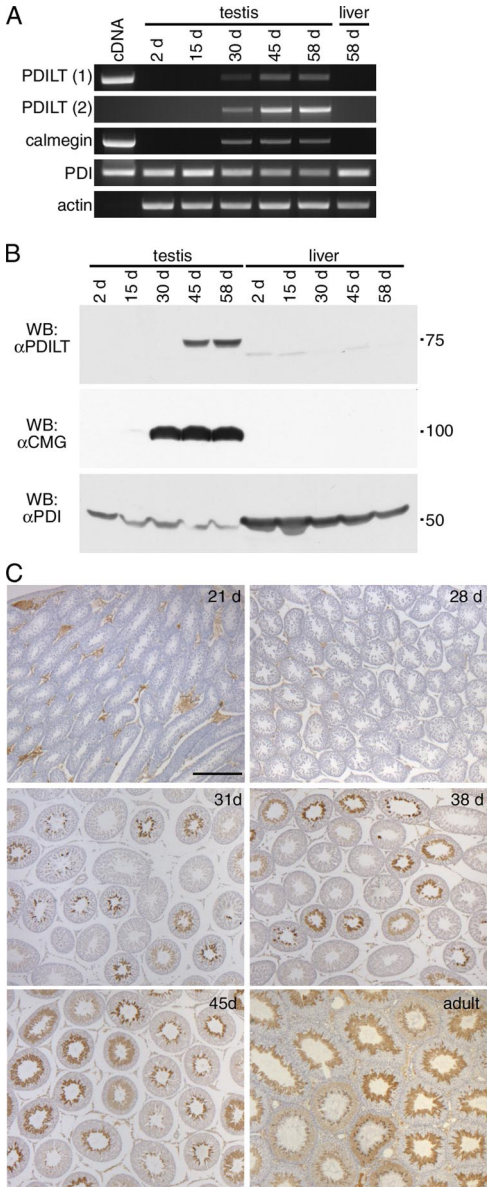

Figure 5. Expression of PDILT commences during the first wave of spermatogenesis. (A) Total RNA extracted from testis of 2-, 15-, 30-, 45-, and 58-d-old rats was used for RT-PCR using primer sets specific for PDILT, calmegin, PDI, and actin. As a positive control, cDNA was used for PDILT, calmegin, and PDI. PDILT primer set 1 was designed on 2 internal exons, whereas PDILT primer set 2 was designed on the first and last exons, to exclude expression of alternatively spliced variants during development. (B) Testis and liver from 2-, 15-, 30-, 45-, and 58-d-old rats were lysed and analyzed by Western blotting for PDILT, calmegin, and PDI. (C) Testis sections from 21-, 28-, 31-, 38-, 45-d-old and adult rats were counterstained with hematoxylin (blue) and immunostained for PDILT (brown).

1). Similar results were obtained when using a second primer set that spanned the entire PDILT coding sequence (Figure 5A, PDILT 2), confirming that expression of PDILT mRNA starts between days 16 and 30. Note the absence of product from the cDNA with this second primer set, as these primers were designed outside the coding region contained in the cDNA. There were no additional products in any of the RT-PCRs on rat testes or liver with these primers, showing that there are no alternative PDILT splicing products. The developmentally regulated expression of PDILT contrasts with the expression of PDI, as PDI mRNA was present in testis and liver of rats throughout postnatal development (Figure 5A).

We also compared the expression of PDILT with that of calmegin, a testis-specific homologue of the chaperone calnexin. Calmegin is expressed in differentiating male germ cells upon the appearance of pachytene spermatocytes (Watanabe *et al.*, 1994). RT-PCR showed that calmegin is readily detected in testis from day 30 onward, consistent with the presence of pachytene spermatocytes at this age (Figure 5A).

To determine the relationship between mRNA levels and protein expression, testes and liver from rats were lysed and analyzed by Western blotting. PDILT was completely absent in testes from 2- and 15-d-old rats. Consistent with the RT-PCR results, PDILT could be detected at day 30 (on very

long exposures, data not shown) and reached adult levels of expression by day 45. (Figure 5B). Calmegin reached adult levels of expression by day 30, whereas PDI was expressed throughout postnatal development (Figure 5B). To examine whether the onset of PDILT expression corresponds with the first appearance of round spermatids in development, sections of testes from rats of different ages were taken for immunohistochemistry. PDILT was not detected in any somatic cells or germ cells in testis from 21- and 28-d-old rats. On day 31, some of the seminiferous tubules contained PDILT-positive cells close to the tubule lumen. The proportion of seminiferous tubules containing PDILT-positive cells dramatically increased with age and by day 45, all of the seminiferous tubules were positive for PDILT (Figure 5C). Taken together, these data show that PDILT expression is detected in testis from 30-d-old rats, consistent with the appearance of round spermatids during the first spermatogenic wave at puberty. This strongly suggests that PDILT is under developmental control and has a role in sperm differentiation.

PDILT Is a Calmegin-interacting Protein

To understand PDILT behavior and function in the ER, we investigated whether any PDILT-protein interactions could be detected, either in transfected cells or in testis tissue. As some thioredoxin family members (Zhao *et al.,* 2003) and redox enzymes (Dias-Gunasekara *et al.,* 2005) form homodimers, we first explored whether PDILT is able to self-associate. Given that spermatids are difficult to isolate and transfect, PDILT-myc and an HA-tagged version were expressed in HeLa cells, either alone or together. Cell lysates were subjected to immunoprecipitation with anti-myc or anti-HA antibodies and analyzed by reducing SDS-PAGE and Western blotting. Both PDILT-myc and PDILT-HA were expressed as expected (Figure 6, lanes 1–3) and anti-myc and anti-HA antibodies pulled down PDILT-myc and PDILT-HA, respectively (Figure 6, lanes 5 and 7, top panel, and lanes 10 and 11, bottom panel) showing that immunoprecipitations were successful. Anti-myc and anti-HA also coimmunoprecipitated PDILT-HA and PDILT-myc, respectively, from double transfectants (Figure 6, lane 7, bottom panel, and lane 11, top panel), indicating that PDILT-myc and PDILT-HA interacted. Anti-myc and anti-HA did not directly immunoprecipitate PDILT-HA and PDILT-myc (Figure 6, lane 6, bottom panel, and lane 9, top panel), demonstrating the specificity of the immunoprecipitations. In addition, the interaction did not occur postlysis because no interaction could be detected when lysates of single transfectants were mixed (data not shown). To determine whether PDILT homodimers are disulfide-linked, we coexpressed PDILT-HA with PDILT-myc C135A/C420A that lacks cysteines and is therefore unable to form mixed disulfides. Anti-myc and anti-HA coimmunoprecipitated PDILT-HA and PDILT-myc C135/C420 (Figure 6, lane 8, bottom panel, and lane 12, top panel), showing that the interaction was not disulfide-linked. Thus, in addition to forming disulfide-linked complexes (Figure 1E), PDILT can engage with itself in a noncovalent complex.

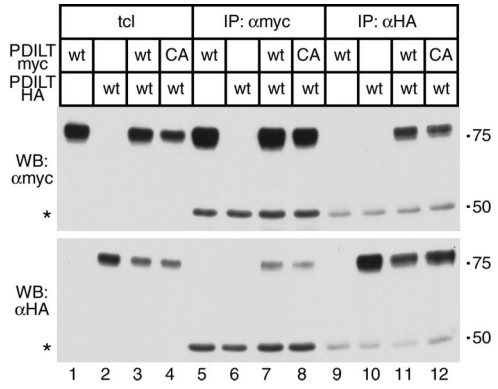

Figure 6. PDILT self-associates. Wild-type (wt) or cysteine mutant (C135A/C420A, denoted CA) HA- or myc-tagged PDILT was expressed in HeLa cells as indicated. Lysates were directly analyzed (lanes 1–4) or subjected to immunoprecipitation with anti-myc (lanes 5–8) or anti-HA (lanes 9–12) before SDS-PAGE and Western blotting with anti-HA (bottom panel) and anti-myc (top panel). The asterisk indicates the bands for the antibodies used for the immunoprecipitations.

We next analyzed endogenous PDILT-protein interactions in testis tissue. The onset of expression and the staining pattern of PDILT resembles that of calmegin (Figure 5). Because both proteins are testis-specific homologues of ubiquitously expressed counterparts involved in protein folding, we explored the possibility that PDILT and calmegin interacted. Testis and liver lysates were either directly analyzed or subjected to immunoprecipitation with anti-PDILT or anti-calmegin, followed by Western blotting for PDILT and calmegin. Both PDILT and calmegin are present in testis, but not in liver (Figure 7A, lanes 1 and 2). The antisera against PDILT and calmegin immunoprecipitated PDILT (Figure 7A, lane 4, top panel) and calmegin (Figure 7A, lane 6, bottom panel), respectively. Significantly, PDILT interacted with calmegin (Figure 7A, lane 6, top panel) and vice versa, calmegin coimmunoprecipitated, albeit more weakly, with PDILT (Figure 7A, lane 4, bottom panel). Anti-calmegin did not directly immunoprecipitate PDILT from a HeLa PDILT-myc lysate, showing the specificity of the immunoprecipitation (Figure 7B). The interaction between the testis proteins PDILT and calmegin is specific as neither PDI (Figure 7C, lane 6, WB αCMG and lane 4, WB: αPDI) nor ERp57 (Figure 7C, lane 4, WB: αERp57) could be detected in calmegin immunoprecipitates from testis lysates.

The PDILT-Calmegin Interaction Is Glycan-independent

Both calnexin and calmegin interact with nascent glycoproteins in a glycan-dependent way (Ikawa *et al.,* 1997). Because PDILT itself is glycosylated, PDILT could be one of these glycoproteins requiring assistance from calmegin to fold. Alternatively, PDILT could be a novel, nonredox active partner for calmegin. To distinguish between these possibilities, mouse liver and testis lysates were mock-treated or treated with endoH to remove glycans. EndoH treatment resulted in an increased electrophoretic mobility of PDILT, consistent with the removal of the PDILT glycans (Figure 7D, lanes 3 and 4, top panel) and confirming that endogenous PDILT is an ER-resident protein (van Lith *et al.,* 2005). Calmegin is not glycosylated, and its mobility remained unchanged upon endoH treatment (Figure 7D, lanes 3 and 4, bottom panel). Deglycosylation had no effect on the efficiency of immunoprecipitation of PDILT or calmegin (Figure 7D, lanes 7 and 8, top panel, and lanes 11 and 12, bottom panel). The anti-calmegin and anti-PDILT antisera coimmunoprecipitated PDILT and, more weakly, calmegin, respectively, from both mock- and endoH-treated samples (Figure 7D, lanes 11 and 12, and 7 and 8), indicating that the calmegin/PDILT interaction was glycan-independent. These results suggest that PDILT is not merely a substrate for calmegin, but rather a partner for this lectin-like protein. The postmeiotic cells of the testes therefore host a unique ER chaperone complex,

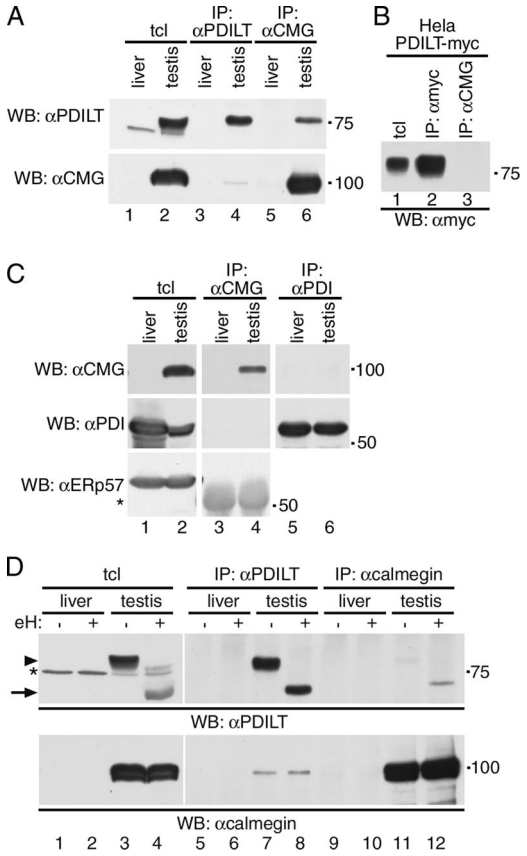

Figure 7. PDILT interacts with calmegin. (A) Lysates from mouse liver and testis were either directly analyzed (lanes 1 and 2) or subjected to immunoprecipitation with anti-PDILT (lanes 3 and 4) or anti-calmegin (lanes 5 and 6) before analysis by SDS-PAGE and Western blotting with anti-PDILT (top panel) and anti-calmegin (bottom panel). (B) Lysates from HeLa cells transfected with PDILT-myc were directly analyzed (lane 1) or subjected to immunoprecipitation with anti-myc (lane 2) and anti-calmegin (lane 3). All samples were analyzed by SDS-PAGE and Western blotting with anti-myc. (C) Lysates from rat liver and testis were either directly analyzed (lanes 1 and 2) or subjected to immunoprecipitation with anti-calmegin (lanes 3 and 4) or anti-PDI (lanes 5 and 6) before analysis by SDS-PAGE and Western blotting with anti-calmegin, anti-PDI (mouse monoclonal), and anti-ERp57. The asterisk indicates cross-reactive antibodies used for the immunoprecipitation in lanes 3 and 4. (D) Lysates from mouse liver and testis were treated with endoH and either directly analyzed (lanes 1–4) or subjected to immunoprecipitation with anti-PDILT (lanes 5–8) or anti-calmegin (lanes 9–12) before analysis by SDS-PAGE and Western blotting with anti-PDILT (top panel) and anti-calmegin (bottom panel). The arrowhead indicates glycosylated PDILT, and the arrow indicates deglycosylated PDILT. The asterisk indicates a background band occasionally observed.

distinct from the redox-active ERp57-calnexin and BiP-PDI partnerships observed for glycoprotein folding in somatic cells (Molinari and Helenius, 2000).

DISCUSSION

The coordination of protein folding in the ER of different tissues in vivo is not well characterized. It has recently become apparent that the physiology of tissue-specific folding, misfolding, and quality control will be central to diseases including those of the pancreas (e.g., diabetes; Ozcan *et al.*, 2006) and the CNS (e.g., Alzheimer's Disease; Uehara *et al.*, 2006). The testes present a special case for the control of ER protein folding because of the unusual environment; besides experiencing low temperature, developing germ cells also require a new proteome and extensive organelle remodeling to produce the acrosome for sperm–egg fusion.

We have used a range of methods to determine the expression of an unusual, testis-specific, PDI homologue, PDILT. PDILT is exclusively found in postmeiotic germ cells (Figure 3A), an expression pattern that is conserved in mouse, rat, marmoset, macaque, and human (Figure 3, A and B). This is in dramatic contrast to other members of the PDI protein family, including ERp57, ERp72, and PDI, which are expressed in all cell types of the testis (Figure 3C). PDILT was not detected in testes at 21 or 28 d of life, at a time when the most mature germ cell type was the pachytene spermatocyte (Clermont and Perey, 1957), but PDILT was detectable in testicular extracts and in cells near the lumen of seminiferous tubules by day 30 or 31, a time when the most mature germ cell types are haploid round spermatids (Figure 4). Thus PDILT seems to be required during spermiogenesis when round spermatids differentiate into mature spermatozoa. These dramatic morphological changes are accompanied by the appearance of many transcripts unique to this cell type, a number of which are also translationally regulated (Hecht, 1990). Proteins unique to the haploid germ cells include testis-specific histones, transition proteins and protamines, all of which are essential for the correct packaging of DNA into the sperm head (Yu *et al.*, 2000; Adham *et al.*, 2001) and proteins essential for the formation of the acrosome (Hurst *et al.*, 1998) and flagellum (Brohmann *et al.*, 1997). Male haploid germ cells also often express genes that are variants of somatically expressed genes (Lin and Morrison-Bogorad, 1991; Hecht, 1998), and PDILT and calmegin may represent such examples.

PDILT shows the same domain architecture as PDI, ERp57, and PDIp (Ellgaard and Ruddock, 2005), but has a number of significant differences. Most notably, PDILT lacks three of the four active site cysteine residues and other residues required for redox activity, such as the equivalent to R120 in PDI (Lappi *et al.*, 2004). It is therefore not surprising that PDILT is not catalytically active as a thiol-disulfide oxidoreductase in any of the standard in vitro assays. However, human PDILT does have two surface-exposed cysteine residues, and these mediate distinct mixed disulfide complexes in cells (Figure 1E). In addition, PDILT does form complexes with the peptide Δ-somatostatin (Figure 1G) and the nonnative protein BPTI (data not shown). Because both nonnative BPTI and PDILT are soluble in isolation but quickly form aggregates when combined, the interaction between these proteins must result in a significant conformational change in at least one of them, probably caused by PDILT binding to hydrophobic residues in BPTI with subsequent exposure of other hydrophobic residues. PDI has three distinct substrate-binding sites (Koivunen *et al.*, 2005) and does not form aggregates in vitro, whereas ERp57 has one of these sites specialized for the interaction with calreticulin/calnexin (Russell *et al.*, 2004) and does form aggregates in vitro with nonnative BPTI and other nonnative proteins (Karala and Ruddock, unpublished observation). PDILT forms a complex with calmegin (Figure 7), consistent with in vitro aggregation occurring to the PDI-family members that are part of a lectin complex in vivo.

Although an indirect interaction between PDILT and calmegin cannot be formally excluded, the association be-

tween the two proteins in the ER of spermatids is glycan-independent (Figure 7). Thus, PDILT is not just a glycosylated substrate for calmegin, but is more likely to be a partner in a unique protein-folding system. Our inability to detect calmegin-ERp57 and calmegin-PDI complexes in testis suggests that the PDILT-calmegin complex performs a unique role in ER quality control, although some caution is required in interpreting negative immunoprecipitation data (Figure 7C). Because PDILT has no oxido-reductase activity in vitro and lacks the classical WCGHC motif of standard oxidoreductases, it is likely that PDILT operates as a folding assistant for spermatid-specific glycoproteins that have been ensnared by calmegin. This is supported by the observation that calmegin interacts with nascent glycoproteins (Ikawa *et al.*, 1997) and our finding that PDILT interacts in vitro with the model peptide Δ-somatostatin and the nonnative protein BPTI (Figure 1). The fact that PDILT can be recovered in disulfide dependent complexes from transfected cells (Figure 1E) and as complexes from testes (van Lith *et al.*, 2005) suggests that both PDILTs solvent-exposed cysteine residues may trap free single cysteines in substrates, perhaps using them as a molecular handle to facilitate protein folding of the peptide backbone. Whether noncovalent PDILT-PDILT complexes (Figure 6) have an independent functional role in vivo, or perhaps operate as an inactive chaperone reservoir, requires further investigation. Together, our work identifies a new quality control hub unique to the ER of spermatids, alongside the ERp57/calnexin and BiP/PDI partnerships found in somatic cells (Molinari and Helenius, 2000). Although calnexin presents nonnative glycoproteins to the redox-active ERp57, the glycan recognition is decoupled from the redox activity for the PDILT/calmegin pair. It will now be important to determine whether calmegin and PDILT work on similar or independent substrates to ERp57 and PDI, given that both PDI and ERp57 are also expressed in postmeiotic cells (Figure 3C). Now that approaches to determine the substrate specificity of ERp57 have been successful (Jessop *et al.*, 2007), it should be possible to identify the range of endogenous PDILT substrates by proteomics and the in vivo role of PDILT homodimerization (Figure 6), once the limitations of transfecting and culturing germ cells have been overcome.

Another interesting possibility is that PDILT is required for specific events during meiosis, such as remodeling the ER in preparation for acrosome formation and the expulsion of the cytoplasmic body. Both PDI and ERp29 are involved in ERAD of microbial proteins (Tsai and Rapoport, 2002; Magnuson *et al.*, 2005), and it may be that PDILT is required for unfolding and retrotranslocation of ER proteins during the programmed disposal of the residual body. Furthermore, ERp57 is found at the surface of sperm and is required for disulfide bond exchange in preparation for gamete fusion (Ellerman *et al.*, 2006). The C-terminal QEDL motif of ERp57 is inefficiently retrieved by the KDEL receptors, meaning that ERp57 may be more reliant on its association with ER-resident proteins for its retention than other PDIs (Raykhel, Alananen, and Ruddock, unpublished data). Thus one possibility is that PDILT regulates ERp57 export to the cell surface by competing with ERp57 for calmegin and calnexin and allowing monomeric ERp57 to be exported from the ER. In vitro experiments with the purified, glycosylated components will be required to determine the relative affinities of these proteins for each other.

Calmegin is required for fertility (Ikawa *et al.*, 1997), and it will be important to determine whether PDILT-deficient mice are also infertile. With many human male infertility cases unexplained, identifying genes and pathways associated with infertility remains a public health priority.

ACKNOWLEDGMENTS

We thank Laura Walters, David Dixon, and Helen McPhee for technical assistance and Neil Bulleid, Lars Ellgaard, Ineke Braakman, and Yoshitake Nishimune for reagents.

REFERENCES

Adham, I. M., Nayernia, K., Burkhardt-Gottges, E., Topaloglu, O., Dixkens, C., Holstein, A. F., and Engel, W. (2001). Teratozoospermia in mice lacking the transition protein 2 (Tnp2). Mol. Hum. Reprod. *7*, 513–520.

Alanen, H. I., Williamson, R. A., Howard, M. J., Hatahet, F. S., Salo, K. E., Kauppila, A., Kellokumpu, S., and Ruddock, L. W. (2006). ERp27, a new non-catalytic endoplasmic reticulum-located human protein disulfide isomerase family member, interacts with ERp57. J. Biol. Chem. *281*, 33727–33738.

Anelli, T., Alessio, M., Mezghrani, A., Simmen, T., Talamo, F., Bachi, A., and Sitia, R. (2002). ERp44, a novel endoplasmic reticulum folding assistant of the thioredoxin family. EMBO J. *21*, 835–844.

Benham, A. M., Cabibbo, A., Fassio, A., Bulleid, N., Sitia, R., and Braakman, I. (2000). The CXXCXXC motif determines the folding, structure and stability of human Ero1-Lalpha. EMBO J. *19*, 4493–4502.

Brohmann, H., Pinnecke, S., and Hoyer-Fender, S. (1997). Identification and characterization of new cDNAs encoding outer dense fiber proteins of rat sperm. J. Biol. Chem. *272*, 10327–10332.

Cai, H., Wang, C. C., and Tsou, C. L. (1994). Chaperone-like activity of protein disulfide isomerase in the refolding of a protein with no disulfide bonds. J. Biol. Chem. *269*, 24550–24552.

Clermont, Y., Morales, C., and Hermo, L. (1987). Endocytic activities of Sertoli cells in the rat. Ann. NY Acad. Sci. *513*, 1–15.

Clermont, Y., and Perey, B. (1957). Quantitative study of the cell population of the seminiferous tubules in immature rats. Am. J. Anat. *100*, 241–267.

Desilva, M. G., Lu, J., Donadel, G., Modi, W. S., Xie, H., Notkins, A. L., and Lan, M. S. (1996). Characterization and chromosomal localization of a new protein disulfide isomerase, PDIp, highly expressed in human pancreas. DNA Cell Biol. *15*, 9–16.

Dias-Gunasekara, S., Gubbens, J., van Lith, M., Dunne, C., Williams, J. A., Kataky, R., Scoones, D., Lapthorn, A., Bulleid, N. J., and Benham, A. M. (2005). Tissue-specific expression and dimerization of the endoplasmic reticulum oxidoreductase Ero1beta. J. Biol. Chem. *280*, 33066–33075.

Dick, T. P., Bangia, N., Peaper, D. R., and Cresswell, P. (2002). Disulfide bond isomerization and the assembly of MHC class I-peptide complexes. Immunity *16*, 87–98.

Ellerman, D. A., Myles, D. G., and Primakoff, P. (2006). A role for sperm surface protein disulfide isomerase activity in gamete fusion: evidence for the participation of ERp57. Dev. Cell. *10*, 831–837.

Ellgaard, L., and Ruddock, L. W. (2005). The human protein disulphide isomerase family: substrate interactions and functional properties. EMBO Rep. *6*, 28–32.

Ferrari, D. M., Nguyen Van, P., Kratzin, H. D., and Soling, H. D. (1998). ERp28, a human endoplasmic-reticulum-lumenal protein, is a member of the protein disulfide isomerase family but lacks a CXXC thioredoxin-box motif. Eur. J. Biochem. *255*, 570–579.

Forster, M. L., Sivick, K., Park, Y. N., Arvan, P., Lencer, W. I., and Tsai, B. (2006). Protein disulfide isomerase-like proteins play opposing roles during retrotranslocation. J. Cell Biol. *173*, 853–859.

Gunther, R., Srinivasan, M., Haugejorden, S., Green, M., Ehbrecht, I. M., and Kuntzel, H. (1993). Functional replacement of the *Saccharomyces cerevisiae* Trg1/Pdi1 protein by members of the mammalian protein disulfide isomerase family. J. Biol. Chem. *268*, 7728–7732.

Hecht, N. B. (1990). Regulation of 'haploid expressed genes' in male germ cells. J. Reprod. Fertil. *88*, 679–693.

Hecht, N. B. (1998). Molecular mechanisms of male germ cell differentiation. Bioessays *20*, 555–561.

Hess, R. A. (1990). Quantitative and qualitative characteristics of the stages and transitions in the cycle of the rat seminiferous epithelium: light microscopic observations of perfusion-fixed and plastic-embedded testes. Biol. Reprod. *43*, 525–542.

Holmgren, A. (1979). Thioredoxin catalyzes the reduction of insulin disulfides by dithiothreitol and dihydrolipoamide. J. Biol. Chem. *254*, 9627–9632.

Hurst, S., Howes, E. A., Coadwell, J., and Jones, R. (1998). Expression of a testis-specific putative actin-capping protein associated with the developing acrosome during rat spermiogenesis. Reprod. Dev. *49*, 81–91.

Ikawa, M., Wada, I., Kominami, K., Watanabe, D., Toshimori, K., Nishimune, Y., and Okabe, M. (1997). The putative chaperone calmegin is required for sperm fertility. Nature *387*, 607–611.

Jessop, C. E., Chakravarthi, S., Garbi, N., Hammerling, G. J., Lovell, S., and Bulleid, N. J. (2007). ERp57 is essential for efficient folding of glycoproteins sharing common structural domains. EMBO J. *26*, 28–40.

Klappa, P., Ruddock, L. W., Darby, N. J., and Freedman, R. B. (1998a). The b′ domain provides the principal peptide-binding site of protein disulfide isomerase but all domains contribute to binding of misfolded proteins. EMBO J. *17*, 927–935.

Klappa, P., Stromer, T., Zimmermann, R., Ruddock, L. W., and Freedman, R. B. (1998b). A pancreas-specific glycosylated protein disulphide-isomerase binds to misfolded proteins and peptides with an interaction inhibited by oestrogens. Eur. J. Biochem. *254*, 63–69.

Koivu, J., Myllyla, R., Helaakoski, T., Pihlajaniemi, T., Tasanen, K., and Kivirikko, K. I. (1987). A single polypeptide acts both as the beta subunit of prolyl 4-hydroxylase and as a protein disulfide-isomerase. J. Biol. Chem. *262*, 6447–6449.

Koivunen, P., Salo, K. E., Myllyharju, J., and Ruddock, L. W. (2005). Three binding sites in protein-disulfide isomerase cooperate in collagen prolyl 4-hydroxylase tetramer assembly. J. Biol. Chem. *280*, 5227–5235.

Kramer, B., Ferrari, D. M., Klappa, P., Pohlmann, N., and Soling, H. D. (2001). Functional roles and efficiencies of the thioredoxin boxes of calcium-binding proteins 1 and 2 in protein folding. Biochem. J. *357*, 83–95.

Kuznetsov, G., Chen, L. B., and Nigam, S. K. (1994). Several endoplasmic reticulum stress proteins, including ERp72, interact with thyroglobulin during its maturation. J. Biol. Chem. *269*, 22990–22995.

Lappi, A. K., Lensink, M. F., Alanen, H. I., Salo, K. E., Lobell, M., Juffer, A. H., and Ruddock, L. W. (2004). A conserved arginine plays a role in the catalytic cycle of the protein disulphide isomerases. J. Mol. Biol. *335*, 283–295.

Lin, S. C., and Morrison-Bogorad, M. (1991). Cloning and characterization of a testis-specific thymosin beta 10 cDNA. Expression in post-meiotic male germ cells. J. Biol. Chem. *266*, 23347–23353.

Lindquist, J. A., Jensen, O. N., Mann, M., and Hammerling, G. J. (1998). ER-60, a chaperone with thiol-dependent reductase activity involved in MHC class I assembly. EMBO J. *17*, 2186–2195.

Magnuson, B., Rainey, E. K., Benjamin, T., Baryshev, M., Mkrtchian, S., and Tsai, B. (2005). ERp29 triggers a conformational change in polyomavirus to stimulate membrane binding. Mol. Cell *20*, 289–300.

Millar, M. R., Sharpe, R. M., Weinbauer, G. F., Fraser, H. M., and Saunders, P. T. (2000). Marmoset spermatogenesis: organizational similarities to the human. Int. J. Androl. *23*, 266–277.

Molinari, M., and Helenius, A. (2000). Chaperone selection during glycoprotein translocation into the endoplasmic reticulum. Science *288*, 331–333.

Morjana, N. A., McKeone, B. J., and Gilbert, H. F. (1993). Guanidine hydrochloride stabilization of a partially unfolded intermediate during the reversible denaturation of protein disulfide isomerase. Proc. Natl. Acad. Sci. USA *90*, 2107–2111.

Oliver, J. D., van der Wal, F. J., Bulleid, N. J., and High, S. (1997). Interaction of the thiol-dependent reductase ERp57 with nascent glycoproteins. Science *275*, 86–88.

Ozcan, U., Yilmaz, E., Ozcan, L., Furuhashi, M., Vaillancourt, E., Smith, R. O., Gorgun, C. Z., and Hotamisligil, G. S. (2006). Chemical chaperones reduce ER stress and restore glucose homeostasis in a mouse model of type 2 diabetes. Science *313*, 1137–1140.

Peltoniemi, M. J., Karala, A. R., Jurvansuu, J. K., Kinnula, V. L., and Ruddock, L. W. (2006). Insights into deglutathionylation reactions. Different intermediates in the glutaredoxin and protein disulfide isomerase catalyzed reactions are defined by the gamma-linkage present in glutathione. J. Biol. Chem. *281*, 33107–33114.

Ruddock, L. W., Freedman, R. B., and Klappa, P. (2000). Specificity in substrate binding by protein folding catalysts: tyrosine and tryptophan residues are the recognition motifs for the binding of peptides to the pancreas-specific protein disulfide isomerase PDIp. Protein Sci. *9*, 758–764.

Ruddock, L. W., Hirst, T. R., and Freedman, R. B. (1996). pH-dependence of the dithiol-oxidizing activity of DsbA (a periplasmic protein thiol:disulphide oxidoreductase) and protein disulphide-isomerase: studies with a novel simple peptide substrate. Biochem. J. *315*(Pt 3), 1001–1005.

Russell, L. D., Ettlin, R., Sinha, A., and Clegg, E. (1990). Histological and Histopathological Evaluation of the Testis, Miami, FL: Cache River Press.

Russell, S. J., Ruddock, L. W., Salo, K. E., Oliver, J. D., Roebuck, Q. P., Llewellyn, D. H., Roderick, H. L., Koivunen, P., Myllyharju, J., and High, S. (2004). The primary substrate binding site in the b′ domain of ERp57 is adapted for endoplasmic reticulum lectin association. J. Biol. Chem. *279*, 18861–18869.

Schaiff, W. T., Hruska, K. A., Jr., McCourt, D. W., Green, M., and Schwartz, B. D. (1992). HLA-DR associates with specific stress proteins and is retained in the endoplasmic reticulum in invariant chain negative cells. J. Exp. Med. *176*, 657–666.

Schulze, W., Riemer, M., Rehder, U., and Hohne, K. H. (1986). Computer-aided three-dimensional reconstructions of the arrangement of primary spermatocytes in human seminiferous tubules. Cell Tissue Res. *244*, 1–7.

Sullivan, D. C., Huminiecki, L., Moore, J. W., Boyle, J. J., Poulsom, R., Creamer, D., Barker, J., and Bicknell, R. (2003). EndoPDI, a novel protein-disulfide isomerase-like protein that is preferentially expressed in endothelial cells acts as a stress survival factor. J. Biol. Chem. *278*, 47079–47088.

Tsai, B., and Rapoport, T. A. (2002). Unfolded cholera toxin is transferred to the ER membrane and released from protein disulfide isomerase upon oxidation by Ero1. J. Cell Biol. *159*, 207–216.

Uehara, T., Nakamura, T., Yao, D., Shi, Z. Q., Gu, Z., Ma, Y., Masliah, E., Nomura, Y., and Lipton, S. A. (2006). S-nitrosylated protein-disulphide isomerase links protein misfolding to neurodegeneration. Nature *441*, 513–517.

van Lith, M., Hartigan, N., Hatch, J., and Benham, A. M. (2005). PDILT, a divergent testis-specific protein disulfide isomerase with a non-classical SXXC motif that engages in disulfide-dependent interactions in the endoplasmic reticulum. J. Biol. Chem. *280*, 1376–1383.

Watanabe, D., Yamada, K., Nishina, Y., Tajima, Y., Koshimizu, U., Nagata, A., and Nishimune, Y. (1994). Molecular cloning of a novel Ca(2+)-binding protein (calmegin) specifically expressed during male meiotic germ cell development. J. Biol. Chem. *269*, 7744–7749.

Weissman, J. S., and Kim, P. S. (1993). Efficient catalysis of disulphide bond rearrangements by protein disulphide isomerase. Nature *365*, 185–188.

Wetterau, J. R., Combs, K. A., Spinner, S. N., and Joiner, B. J. (1990). Protein disulfide isomerase is a component of the microsomal triglyceride transfer protein complex. J. Biol. Chem. *265*, 9800–9807.

Yu, Y. E., Zhang, Y., Unni, E., Shirley, C. R., Deng, J. M., Russell, L. D., Weil, M. M., Behringer, R. R., and Meistrich, M. L. (2000). Abnormal spermatogenesis and reduced fertility in transition nuclear protein 1-deficient mice. Proc. Natl. Acad. Sci. USA *97*, 4683–4688.

Zhao, Z., Peng, Y., Hao, S. F., Zeng, Z. H., and Wang, C. C. (2003). Dimerization by domain hybridization bestows chaperone and isomerase activities. J. Biol. Chem. *278*, 43292–43298.

Zheng, J., and Gilbert, H. F. (2001). Discrimination between native and non-native disulfides by protein-disulfide isomerase. J. Biol. Chem. *276*, 15747–15752.